# DYNAMICS OF CAVEOLIN-1 ON THE PLASMA MEMBRANE

by

Amber Griffith

A thesis submitted to the Faculty of the University of Delaware in partial fulfillment of the requirements for the Bachelor of Arts in Biology with Distinction

Spring 2012

**DYNAMICS OF CAVEOLIN-1 ON THE PLASMA MEMBRANE**

by

Amber Griffith

Approved: _____

Anja Nohe, Ph.D.
Professor in charge of thesis on behalf of the Advisory Committee

Approved: _____

Gary Laverty, Ph.D.
Committee member from the Department of Biological Sciences

Approved: _____

Marlene Emara, Ph.D.
Committee member from the Board of Senior Thesis Readers

Approved: _____

Donald Sparks, Ph.D.
Chair of the University Committee on Student and Faculty Honors

## ACKNOWLEDGMENTS

I would like to thank Dr. Anja Nohe for inviting me to work in her lab. I would like to thank everyone in Dr. Nohe's lab, especially Rachel Schaefer and Jeremy Bonor for all their help and support during my project. I would also like to thank Dr. Marlene Emara and Dr. Gary Laverty for their support and presence in my committee. In addition, I would like to acknowledge the Jeffery Caplan and Kirk Cyzmmek at the Delaware Biotechnology Institute for all of their help. Lastly I would like to thank my family for the moral support they provided and everyone else who helped me along the way.

## TABLE OF CONTENTS

## LIST OF TABLES

## LIST OF FIGURES

## ABSTRACT

Caveolae are important micro-domains that are found on the plasma membrane. Caveolae are known to aid in important cell processes such as endocytosis, cell signaling and cholesterol homeostasis. They are made up of sphingolipids, cholesterol and a protein called caveolin-1, which has two isoforms; caveolin-1α and caveolin-1β. It is currently debatable that these micro-domains are actively moving around on the cell surface. We believe that caveolae are dynamic on the plasma membrane, and the movement that they exhibit is non-random. The purpose of this project was to gain a better understanding of the dynamics of caveolae by studying the protein that it is composed of; caveolin-1α and caveolin-1β. Time lapse photography and confocal microscopy were used to investigate the dynamics of caveolin-1α and caveolin-1β. Diffusion coefficients were also calculated to determine the type of movement the proteins exhibited. The results from our experiments showed that caveolin-1β is more dynamic and temperature-dependent, compared to caveolin-1α, and that both proteins exhibit anomalous diffusion and direct movement with diffusion.

# Chapter 1

## INTRODUCTION

Caveolae are omega-shaped invaginations in the plasma membrane [1, 2]. They are found to form transport vesicles and tubular structures [1, 2]. Caveolae are found on the plasma membrane of many different cells such as fibroblasts, endothelial cells, adipocytes and smooth muscle cells [1-4]. The main component of caveolae is the protein, caveolin. There are about 144 caveolin proteins in each invagination found on the plasma membrane [1, 3]. Three types of caveolin proteins are known to associate in caveolae. They are caveolin-1, caveolin-2 and caveolin-3 [1, 2]. These three proteins take on a hairpin shape and when associated with the plasma membrane, they have both their n-terminus and c-terminus in the cytoplasm of the cells [2-4].

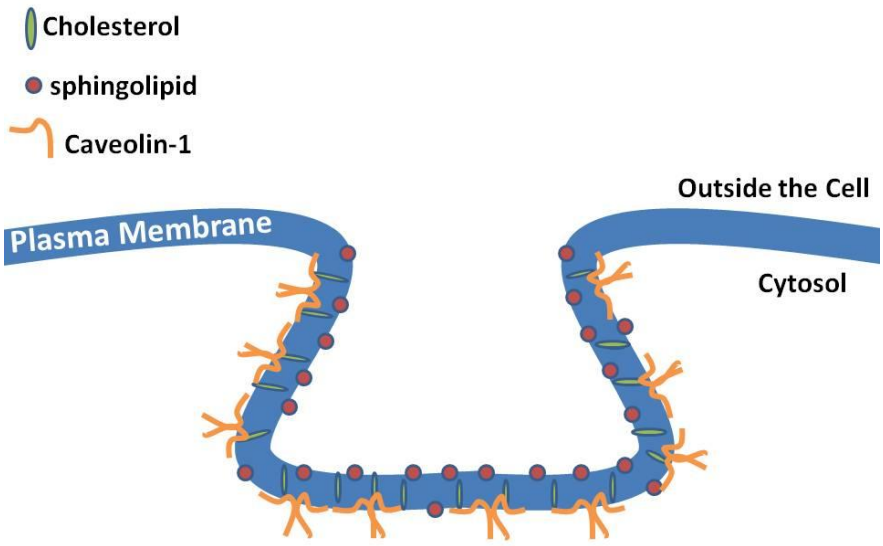


Figure 1.1 Caveolae form an omega-shaped invagination on the plasma membrane. There are a variety of proteins, cholesterol and lipids that are found in these micro-domains.

Either caveolin-1 or caveolin-3 is needed to form the caveolae [2, 5]. Caveolin-1 is known to have two isoforms, α and β [1, 2, 6]. The difference between the two isoforms is a truncation of 31 amino acids from the N- terminus of caveolin-1β and caveolin-1α contains tyrosine 14 which aids in Src phosporylation [1, 4]. Caveolae are composed of a mixture of the two caveolin-1 isoforms or alternatively, only contain the isoform, caveolin-1β [6]. It was found that caveolae that only contain caveolin-1β are shallower in depth, compared to caveolae that contain both α and β isoforms, which suggests a different functionality for each isoform [7].

Caveolin-2 is known to be co-expressed with caveolin-1 [1]. It forms hetero-oligomers with caveolin-1 in order to be targeted to the cell surface [4]. Without the

presence of caveolin-1, caveolin-2 will remain in the Golgi apparatus and it would eventually be degraded [1, 2]. The co-expression of caveolin-1 and caveolin-2 forms caveolae that are deeper in structure [1]. Caveolin-3 is found mostly in muscle cells and it is 27 amino acids shorter than caveolin-1 [1, 2, 4]. Caveolin-3 helps maintain the contractile phenotype of smooth muscle cells and it plays a key role in muscle function and structure[1].

Caveolins are first synthesized in the endoplasmic reticulum using signal recognition particle (SRP) protein synthesis [3]. Caveolin-1 and caveolin-2 are then transported to the Golgi apparatus as monomers, which then associate to form hetero-oligomers between caveolin-1 and caveolin-2 or homo-oligomers with two caveolin-1 proteins [1, 2, 4]. They are able to form oligomers by palmitoylation on cystine residues 133, 143 and 156 in caveolin-1, as well as interactions between the caveolin scaffolding domain (CSD) located near the N-terminus of the caveolin protein [1, 2, 4, 5]. The oligomerization of caveolin is facilitated by cholesterol and sphingolipids while still in the Golgi [1]. The addition of sphingolipids and cholesterol is vital for the transport of caveolin proteins to the plasma membrane from the Golgi apparatus [1-4]. Once on the plasma membrane, the caveolins form a mature caveola that is enriched with cholesterol, sphingolipids and various proteins [1, 6, 8, 9]. The mature caveolae are also known to associate with the cytoskeleton of cells by interacting with microtubules and actin microfilaments [3, 4]. On the cytoplasmic side of caveolae, they are known to have a striated surface [1, 2]

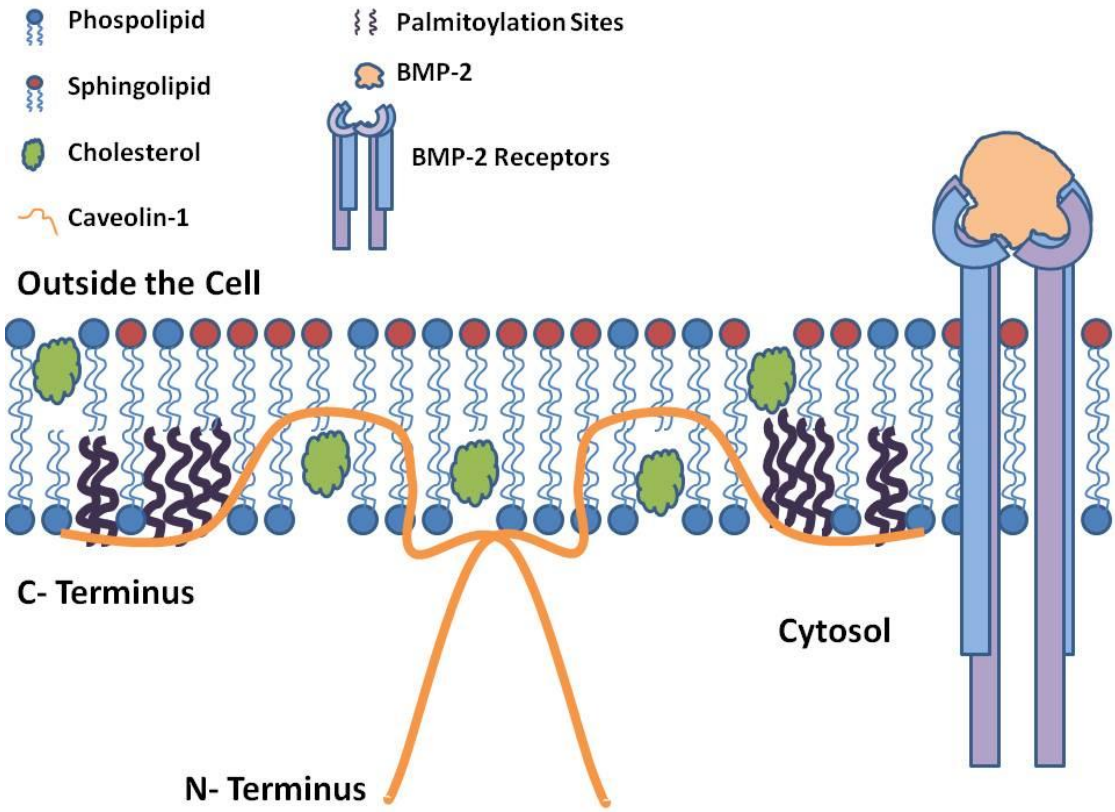


Figure 1.2 Close-up of caveolae. Caveolae are composed of an array of different proteins and lipids. Receptor proteins are also found in this micro-domain. It is found that the outer leaflet of the plasma membrane of caveolae have high concentrations of sphingolipids, compared to the concentration of phospholipids.

Emerging science shows another set of proteins that are important for the formation and function of caveolae [1, 10-12]. These proteins are cavin-1, cavin-2, cavin-3, and cavin-4 and they serve as support proteins for the caveolae [10]. Cavin-1 is capable of recognizing and associating with mature caveolin proteins on the plasma membrane [3]. Cavin-1 and cavin-2 are needed to ensure caveolae formation [4]. They help stabilize the micro-domain at the cell surface [12]. They do this by binding to each other, which in turn sequesters caveolins into the caveolae [10]. Cavin-2 is

also known to aid in generating membrane curvature within caveolae, as well as serving as a substrate for protein kinase C, along with cavin-3, in caveolae signaling [3, 10]. Cavin-3 is known to aid in the formation of caveolar vesicles and it aids in caveolar endocytosis [3, 10]. Like caveolin-3, cavin-4 is restricted to muscle cells [3, 10]. Cavin-4 plays a role in regulating ERK1/2 signaling and myogenesis [3].

There are a number of ways that a cell regulates the formation of caveolae on its cell surface. The presence of cholesterol dictates the formation of caveolae [12]. In cells depleted of cholesterol, caveolins migrate back to the endoplasmic reticulum and Golgi apparatus [2]. Cholesterol positively regulates the formation of caveolae by stabilizing caveolins at the plasma membrane, as well as increasing mRNA templates for caveolin synthesis [5]. There are other biological factors that influence caveolae. The MAP/ERK pathway has been shown to be a negative regulator in the expression of caveolin-1 [5] [Reference]. Other proteins that regulate caveolin expression include protein kinase A (PKA), src family kinases, phospatidylinositol-3 kinase (PI-3K), and protein kinase Cα (PKCα) [5]. Caveolae can also be controlled by non-biological elements. Chemicals such as methyl-β-cyclodexrin, filipin, and nystatin are known to reduce the abundance of caveolae on the plasma membrane, in addition to inhibiting caveolar endocytosis [4].

Caveolae are known to be involved in many cell processes, such as cell signaling, endocytosis, exocytosis, transcytosis, stabilizing the plasma membrane, and cholesterol homeostasis [2, 4, 5, 9, 11]. An example of the role of caveolae in transcytosis is in epithelial cells where caveolae are known to transcytose albumin across the cell [4]. A variety of receptor proteins are known to associate with caveolae. A few examples of these receptors include epidermal growth factor

receptors (EGFR), G-protein subunits, endothelial nitric oxide synthases (eNOS), metabolic glutamine receptor (MGluR1/5) and platelet derived growth factor receptors (PDGFR), [3-5, 8-10]. Caveolae facilitate cell signaling by providing a functional platform and sequestering the receptors within the structure [1, 7]. It sequesters the receptors in the domain by the use of the protein, caveolin-1. The receptors interact with caveolin-1 via the caveolin binding domain (CBD) [5]. When caveolin-1 binds to the targeted receptor, it acts as an inhibiting factor to the signal cascade for that specific protein receptor [4-6]. Nohe *et. al* [7][Reference #] found that the β isoform of caveolin-1 may be responsible for the inhibitory effects of caveolae on specific receptors. Their experiments showed that caveolae enriched in only caveolin-1β had an inhibitory effect on cell signaling, whereas the inhibitory effect was reversed when the composition of the caveolae changed from containing only caveolin-1β to containing a mixture of caveolin-1α and caveolin-1β in the micro-domain [7]. Caveolae keep the receptors in their inactive state until their ligands are present to stimulate them [4, 6, 7].

Caveolae are important for the internalization of specific materials. In primary adipocytes, insulin undergoes rapid internalization via caveolar endocytosis [4]. Caveolar endocytosis is also important in the detachment of cells by aiding in the internalization of integrins [3, 12]. Caveolae are also known to be negative regulators in endocytosis [1, 3, 4, 8]. They do this by stabilizing the micro-domain on the plasma membrane, which in turn delays the internalization of specific materials [1, 3]. When caveolar endocytosis does occur, it is regulated by the presence of cholesterol and GM1-gangliosides at the cell surface, in addition to polymerization of the actin cytoskeleton and the involvement of kinases [1, 3, 4].

The main point of focus for this research project will be the two isoforms of caveolin-1. We hypothesize that caveolae are dynamic on the plasma membrane, and the movement that they exhibit is not random. The goal of the experiment is to gain a better understanding of the function of the micro-domain caveolae. In recent science, there is a disagreement as to whether caveolae are dynamic or immobile structures on the plasma membrane [3, 9]. The dynamics of the two isoforms on the plasma membrane will be captured using confocal microscopy. If caveolae are found to be dynamic on the plasma membrane, steps will then be taken to determine if the movement of this micro-domain is random, gated or guided by a stimulus. By using time lapse imaging and confocal microscopy, we can be one step closer to understanding the dynamics of caveolae, and possibly use this knowledge for clinical implications.

## Chapter 2

## CALIBRATING A TEMPERATURE STAGE

Near the beginning of the project, the confocal microscope that was intended to be used lacked a temperature stage to aid in imaging at 37°C. As a result, the first step of the project was to make a custom built temperature stage to successfully complete the intended experiments.

An aluminum stage was made to fit into the table of the confocal microscope. In this template, a matek dish was able to rest in a compartment while being heated at the same time. Two peltier cooling devices were attached to a 15V 3AMP DC power supply and were used to heat up the aluminum stage on either side. The heating side of the cooling device was set to heat the removable plate that housed the matek dish, while the cooling side of the cooling device was in contact with the insert to keep the stage from reaching the same temperature. The voltage was gradually increased until it successfully maintained 2 mL of distilled water at 37°C for at least 20 minutes. The temperature readings were taken every 5 minutes in the center of the matek dish for a duration of 60 minutes. The optimal voltage for the temperature stage was around 3 volts and 3 amps.

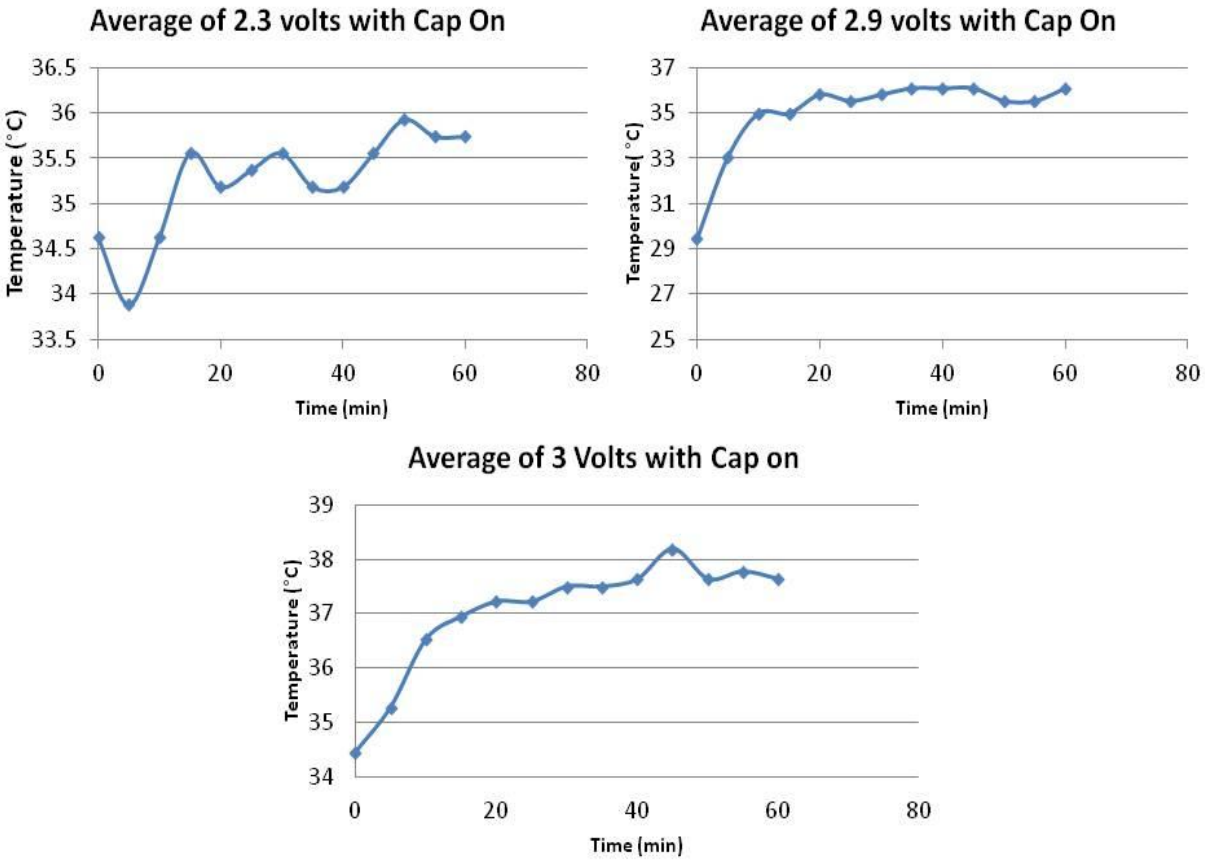


Figure 2 Average of four temperature readings of 2 mL of distilled water heated in the temperature stage at various voltages and 3 amps over a time period of 60 minutes. The readings were taken every five minutes in the center of the dish. (See appendix for tables of raw data)

After the temperature stage was successfully set to keep the media in the matek dish stable at 37°C, the next step was to set the stage to cool down to 4°C. At first, attempts were made to use the cooling side of the peltier cooling device to attain the desired temperature. After several trials, it was conclusive that the cooling side of the

device could not overcome the heat transfer from the heating side. To combat this issue, ice bags were used to cool the aluminum stage to 4°C.

# Chapter 3

# MATERIALS AND METHODS

## 3.1 Cell Culture

Osteoblastic mouse calvaria cells from the mouse line MC3T3-E1 were used for all the transfection experiments. The cells were maintained in Minimal Essential Medium (MEM) Alpha medium, supplemented with 5% fetal bovine serum (FBS, Gemini BioProducts), 1% penicillin-streptomycin (10,000 IU/mL penicillin, 10,000 ug/mL streptomycin Gemini BioProducts) and 1% L-glutamine (200 mM solution, Gemini Bioproducts). Cells were incubated in a humidified atmosphere maintained at 4.5% $CO_2$ and 37°C.

The cells were grown to confluence and split into new flasks to maintain the growth of the cell line. Confluent cells were treated with 10% trypsin phosphate buffer solution (PBS) to detach the cells from the flask. The detached cells were then transferred to a new flask to maintain growth.

## 3.2 Transfection

When the cells were confluent, 10% trypsin-PBS was used to detach the cells. The detached cells were then transferred to matek glass bottom dishes. The dishes were incubated in a humidified atmosphere maintained at 4.5% $CO_2$ and 37°C for 24-48 hours. The media was then removed by vaccum and replaced with serum-free media. The cells were then transfected with 1 μg of caveolin-1α-GFP and 1 μg of

caveolin-1β-GFP in a solution of 286 µl of serum free media and 6 µl of turbofect. Cells were also transfected with 2µg of caveolin-1β in a solution of 286 µl of serum free media and 6 µl of turbofect. The cells sat in the serum-free media with the solution for 4-8 hours in the incubator. The media was then removed by vacuum and replaced with serum-supplemented media.

### 3.3 Confocal Imaging

Time series photographs and still images were taken on a Zeiss 5LIVE high speed confocal microscope. A 100X phase 3 oil immersion lens, along with 488 nm and 560 nm lasers were used for imaging. Whole cell images were taken at 1X zoom (512 x 512 pixels) with the pinholes for the 488 nm laser at 148 µm and the pinholes for the 560 nm laser at 158 µm. The laser power for the 488 nm laser was at 2% and the 560 nm laser power was set for 3%. Close up images were taken at 10X zoom (512 x 512 pixels) with the pinholes for the 488 nm and 560 nm lasers set to 766 µm. The laser power for the two lasers was set at 0.5%. Time series photographs were taken every 10 seconds for a duration of 5 minutes in their respective zooms. Caveolin-1β was viewed in the green panel, and caveolin-1α was viewed in the red panel under the confocal microscope.

### 3.4 Statistical Analysis

The time series photographs were quantified using Volocity software located at the Delaware Biotoechnology Institute. The data extracted from the analysis included the track velocities of caveolae containing caveolin-1α and caveolin-1β separately, the total distance the caveolae travelled for the duration of the time series, as well as the

mean square displacement. The data was then compared to find statistical significance through the use of a two-tailed t-test that assumed equal variance.

# Chapter 4

# RESULTS

## 4.1 Imaging at 25°C

Time series photographs were taken of the cell as a whole and a close up of the plasma membrane on the peripheral section of the cell to visualize the dynamics of caveolin in real-time on living cells. The images were taken over a duration of 5 minutes, where an image was taken every ten seconds. Based on the images taken of the cell as a whole, larger clusters appear to be stationary, while smaller clusters appear to be more mobile. The movement of caveolae appeared to be more noticeable in the green panel (caveolin-1β) than the red panel (caveolin-1α). Similar results were seen when looking at the peripheral sections of the plasma membrane close up. Smaller caveolae were more mobile and there was more activity in the green panel.

The images were then analyzed using Volocity software. Using this software allowed us to quantify the movement of the proteins. The clusters of Caveolin-1 proteins were manually tracked in both the green (caveolin-1β) and red (caveolin-1α) panels separately. The software was able to determine the track velocity (μm/sec), and total distance each cluster traveled over the duration of the time series (μm).

The track velocity, and total distance traveled were then analyzed statistically using a t-test to check for significance. After analyzing the data, the average track velocity of caveolin-1β (green panel) was 0.2071 um/sec. Its average total distance traveled was 2.514 μm. The track velocity of caveolin-1α (red panel) was 0.01549 μm/sec. Its average total distance traveled was 2.279 μm. Based on the statistical t-

test, there was no statistical significance between the total distances traveled by caveolin-1α and caveolin-1β at room temperature. There was a statistical significance between the track velocity of caveolin-1α and caveolin-1β using a two-tailed t-test (see figure 4.1d).

Diffusion coefficients were also calculated to determine the type of movement caveolin-1α and caveolin-1β exhibited. This was done by graphing the mean square displacement as a function of time, and deriving the diffusion coefficient from the line of best fit. When the diffusion coefficients were graphed for both proteins, it appeared that there were two types of movement exhibited. There were two lines of best fit that were prominent throughout the data (see figure 4.1.2). The line of best fit that followed the template of a power equation ( $ax^n$) represented anomalous diffusion, and the line of best fit that followed the polynomial equation ($ax^2 + bx$) represented direct motion with diffusion [13]. The average diffusion coefficient for caveolin-1β that followed the polynomial equation was calculated to be $8.25*(10)^{-12}$ $cm^2$/sec. For caveolin-1β that followed the power equation, the diffusion coefficient was calculated to be $2.13*(10)^{-12}$ $cm^2$/sec (see table 1)

Caveoilin-1α had similar readings for its calculated diffusion coefficient. There were some that followed the power equation and some that followed the polynomial equation. The calculated average diffusion coefficient for caveoli-1α that followed the power equation was $3.78*(10)^{-12}$ $cm^2$/sec and the average diffusion coefficient for caveolin-1α that followed the polynomial equation was calculated to be $4.04*(10)^{-13}$ $cm^2$/sec (see table 1).

Cells transfected only with caveolin-1β were also imaged using time lapse imaging. The images were then analyzed using the velocity software. The average

track velocity and average total distance travelled was calculated to be 0.019 μm/sec and 1.766 μm respectively. The total distance travelled and the average track velocity of the cells that were only transfected with caveolin-1β were significantly lower than the total distance travelled and average tack velocity of caveolin-1β of cells that were transfected with caveolin-1α (see figure 4.1.3b-c).

The diffusion coefficients were calculated for the single transfection. Like the double transfection, there were two types of movement that were prominent; diffusions coefficients that followed the power equation and diffusion coefficients that followed the polynomial equation. The calculated average diffusion coefficients of caveolin-1β that followed the power equation was 4.88*(10)˙12 cm2/sec and the calculated average diffusion coefficient for caveolin-1β that followed the polynomial equation was1.31*$(10)^{-12}$ $cm^2$/sec (see table 1).

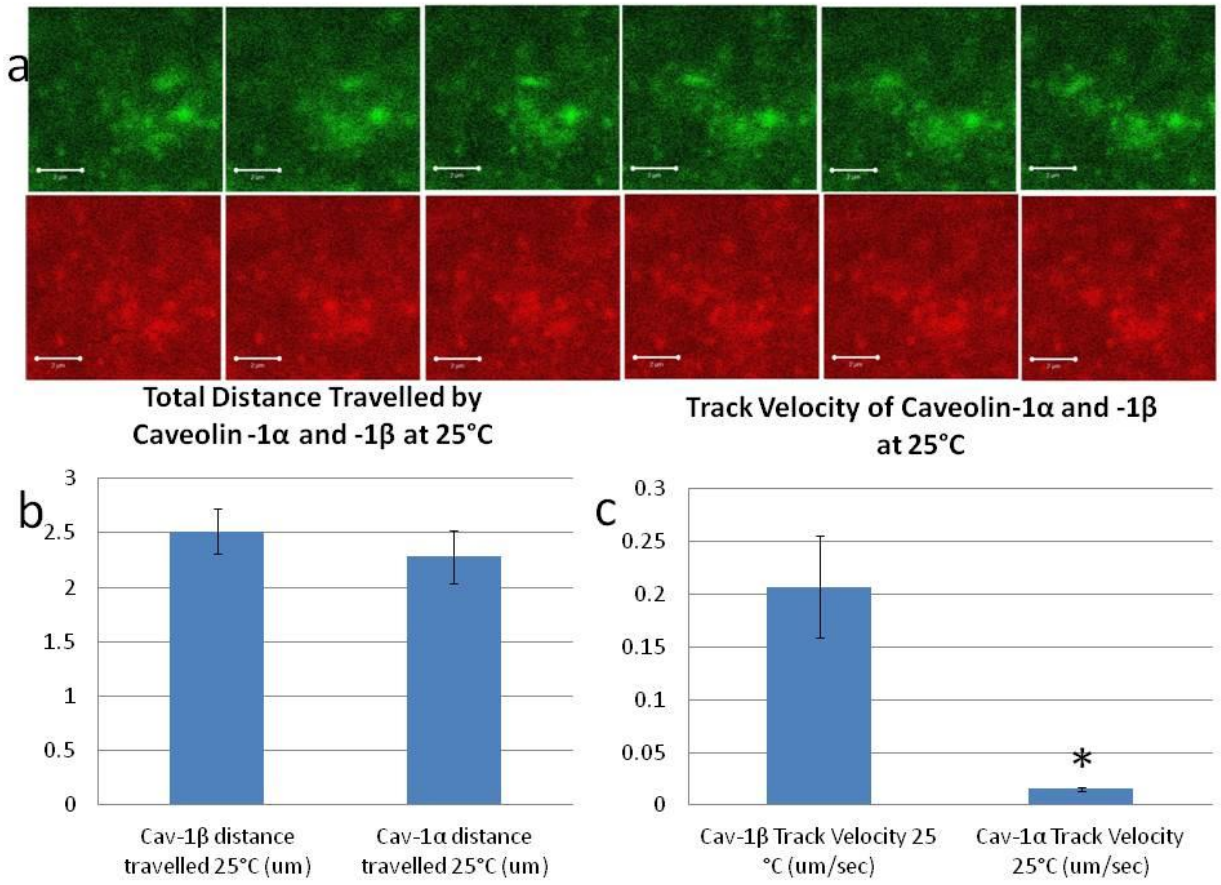


Figure 4.1 (a) Excerpt from a time series photograph. The first image starts at 3 minutes and 30 seconds. The images were taken every ten seconds. The green panel represents caveolin-1β and the red panel represents caveolin-1α. (b) Average total distance travelled of caveolin-1α and caveolin-1β at 25°C. The total distance travelled was calculated separately for each panel using Volocity software. (c) The average track velocity was also calculated separately for each panel using the velocity software. The asterisk represents statistical significance by a two tailed t-test (p value =0.015).

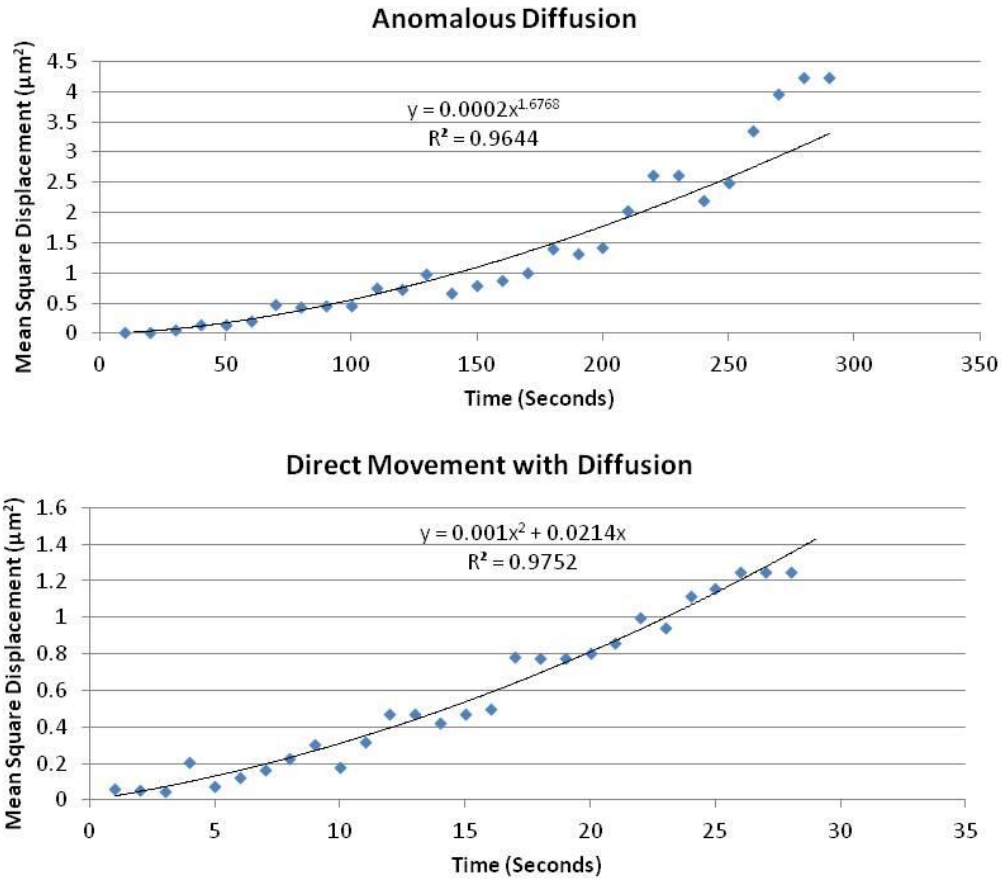


Figure 4.1.2 examples of lines of best fit derived from the graph of mean square displacement over time. Anomalous diffusion represents a non linear relationship between the mean square displacement and time, while the direct movement with diffusion represents that the caveolae are experiencing a drift with a certain velocity (denoted by the constant "a" in the $ax^2$). Since these graphs do not follow a straight line, the movement caveolae exhibit is not random. These graphs are taken of caveolin-1β at 25°C. the $R^2$ value represents how well the line fits the data.

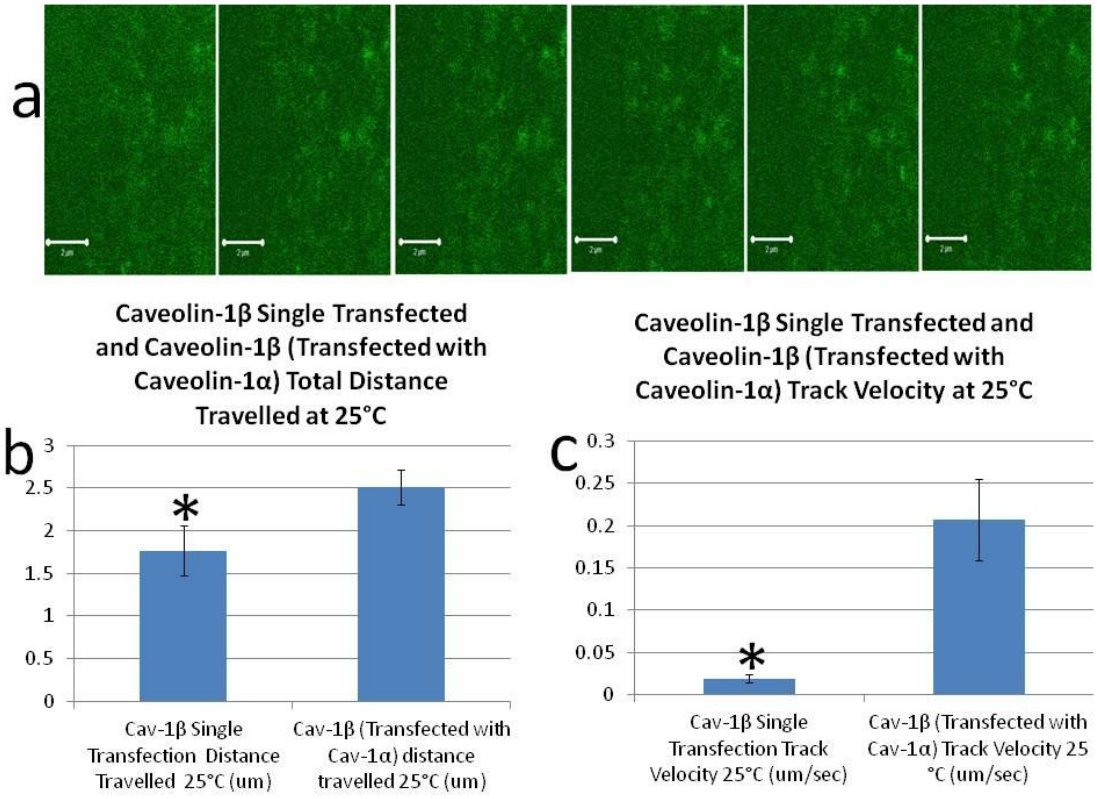


Figure 4.1.3 (a) Excerpt from a time series photograph. The first image starts at 1 minute and 20 seconds. The images were taken every ten seconds. The green panel represents caveolin-1β, which the cells were only transfected with this isoforms of caveolin-1. (b) The average distance traveled was calculated using the velocity software. The asterisk represents statistical significance by a two tailed t-test (p value = 0.042). (c) Average track velocity of caveolin-1β transfected alone and imaged at 25°C. The track velocity was also calculated using Volocity software. The asterisk represents statistical significance by a two tailed t-test (p value = 0.0094).

Table 1: Average diffusion coefficients for caveolin-1α and caveolin-1β. The diffusion coefficients were derived from the line of best fit from a graph of mean square displacement.

| | Caveolin-1β at 25°C | Caveolin-1α at 25°C | Caveolin-1β at 4°C | Caveolin-1α at 4°C | Caveolin-1β Transfected alone at 25°C |
|---|---|---|---|---|---|
| Average Polynomial Diffusion Coefficient ($cm^2$/sec) | $8.22*(10)^{-12}$ | $4.04*(10)^{-12}$ | $7.91*(10)^{-12}$ | $4.10*(10)^{-12}$ | $1.31*(10)^{-12}$ |
| Average Power Diffusion Coefficient ($cm^2$/sec) | $2.13*(10)^{-12}$ | $3.78*(10)^{-12}$ | $1.01*(10)^{-12}$ | $1.42*(10)^{-12}$ | $4.88*(10)^{-13}$ |

### 4.2 Imaging at 4°C

The same process was done to image the cells at 4°C; the only difference was the temperature. Once again, when the cell was imaged as a whole, the larger clusters were mainly stationary, while smaller clusters were more mobile. Visually, there was more movement in the green panel (caveolin-1β), compared to the red panel (caveolin-1α). The same was noted when close up images were taken of the peripheral parts of the cell.

The images for 4°C were also analyzed using Volocity software. The clusters of caveolin-1 proteins were tracked manually in both the green panel (caveolin-1β) and the red panel (caveolin-1α) separately. The track velocity (μm/sec) and total distance traveled through the duration of the time series (μm) was also measured at this temperature.

T-tests were also done on the track velocity, displacement, and displacement rates to check for statistical significance. The total distance traveled for caveolin-1α was calculated to be 2.450 um. The track velocity was calculated to be 0.01150 μm/sec. The track velocity for caveolin-1β was calculated to be 0.0130 μm/sec and its total distance traveled was 2.635 μm.

Based on the t-tests that were done, there was no statistical significance between the total distance travelled between caveolin-1α and caveolin-1β at 4C. The t-test also showed no statistical significance between the track velocity of the two proteins at this temperature (see figure 4.2b and 4.2c).

Diffusion coefficients were also calculated for caveolin-1α and caveolin-1β at 4°C. At this temperature, the results were similar to the results at 25°C, regarding the prominent lines of best fit found in the data. In both caveolin-1α and caveolin-1β, there were some that had a line of best fit that followed the power equation and others that had a line of best fit that followed the polynomial equation. For caveolin-1β, the calculated average diffusion coefficient for the polynomial equation was $7.91*(10)^{-12}$ $cm^2/sec$, and the calculated average diffusion coefficient for the power equation was $1.01*(10)^{-12}$ $cm^2/sec$ (see table 1).

Like caveolin-1β, when the diffusion coefficients were derived for caveolin-1α, there were some that followed the power equation and others that followed the polynomial equation (see figure 4.1.2). The average diffusion coefficient for caveolin-1α that followed the polynomial equation was $4.10*(10)^{-12}$ $cm^2/sec$ and the average diffusion coefficient for caveolin-1α that followed the power equation was calculated to be $1.42*(10)^{-12}$ $cm^2/sec$ (see table 1).

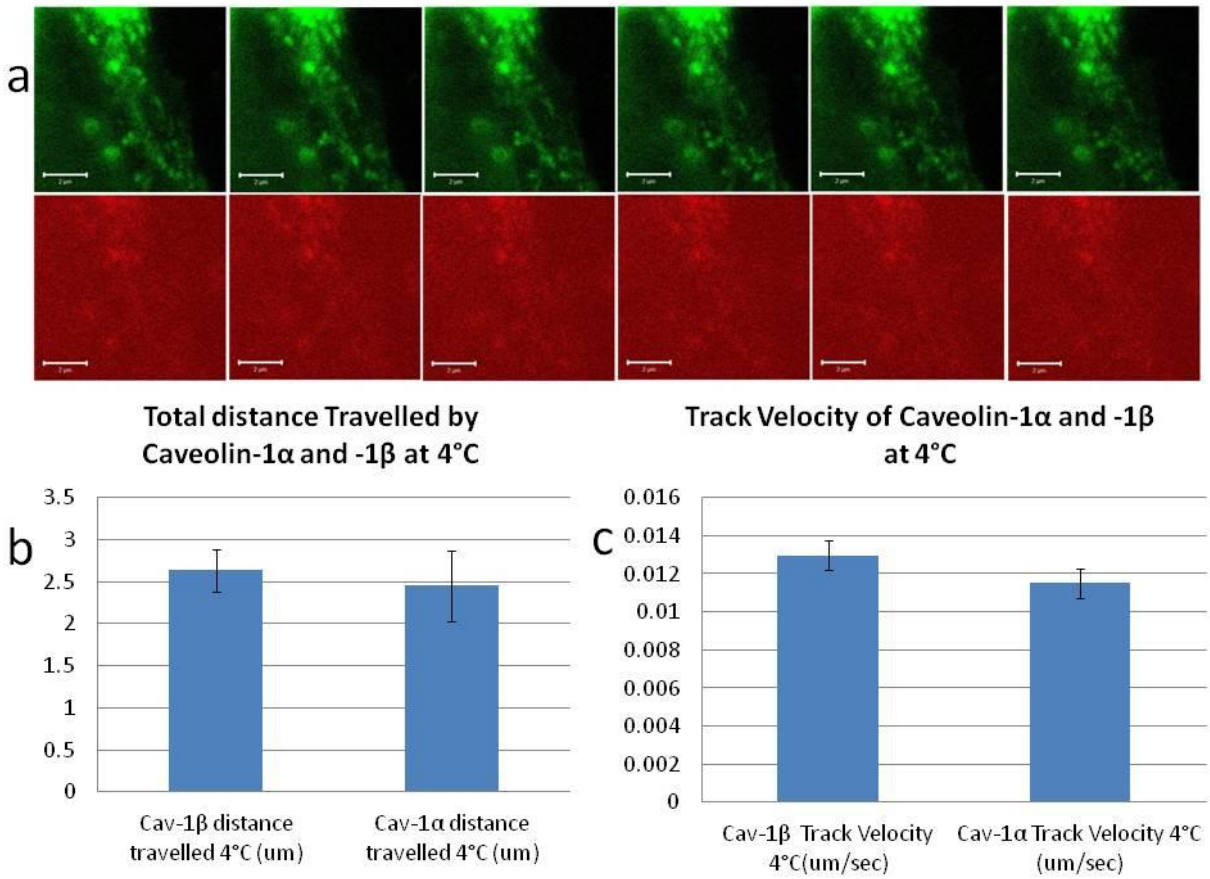


Figure 4.2 (a) Excerpt from a time series photograph. The first image starts at 1 minute. The images were taken every ten seconds. The green panel represents caveolin-1β and the red panel represents caveolin-1α. (b) Average total distance travelled of caveolin-1α and caveolin-1β at 4°C. The total distance travelled was calculated separately for each panel using Volocity software. (c) The average track velocity was also calculated separately for each panel using the velocity software.

### 4.3 Imaging at 37°C

When experiments were initiated to image the cells at 37°C, the lab discovered that there was a contamination issue. The contaminant was determined to be mycoplasma, a type of bacteria well known for contaminating cell cultures. Once the

contamination was recognized, all cell cultures and media were discarded. The cell culture room was sterilized by wiping down all surfaces with 70% ethanol solution. The incubator that housed the cells was taken apart and removable parts were autoclaved and then wiped down with 70% ethanol solution. Due to the timing of the contamination, I was unable to successfully image my cells at 37°C.

### 4.4 Comparing Caveolin-1α and Caveolin-1β between 4°C and 25°C

After the data were analyzed for 4°C and 25°C, the results were compared using t-tests to see if there was any statistical significance between the two temperatures. Based on the t-tests done, no statistical significance was found between the average distance traveled between caveolin-1α and caveolin-1β at both temperatures.

When comparing the track velocities, the t-tests showed a statistical significance between the track velocity of caveolin-1β at 4°C and 25°C (see figure 4.4c). There was also a statistical significance between the track velocity of caveolin-1α and caveolin-1β at 25°C (see figure 4.1d). The other comparisons showed no statistical significance.

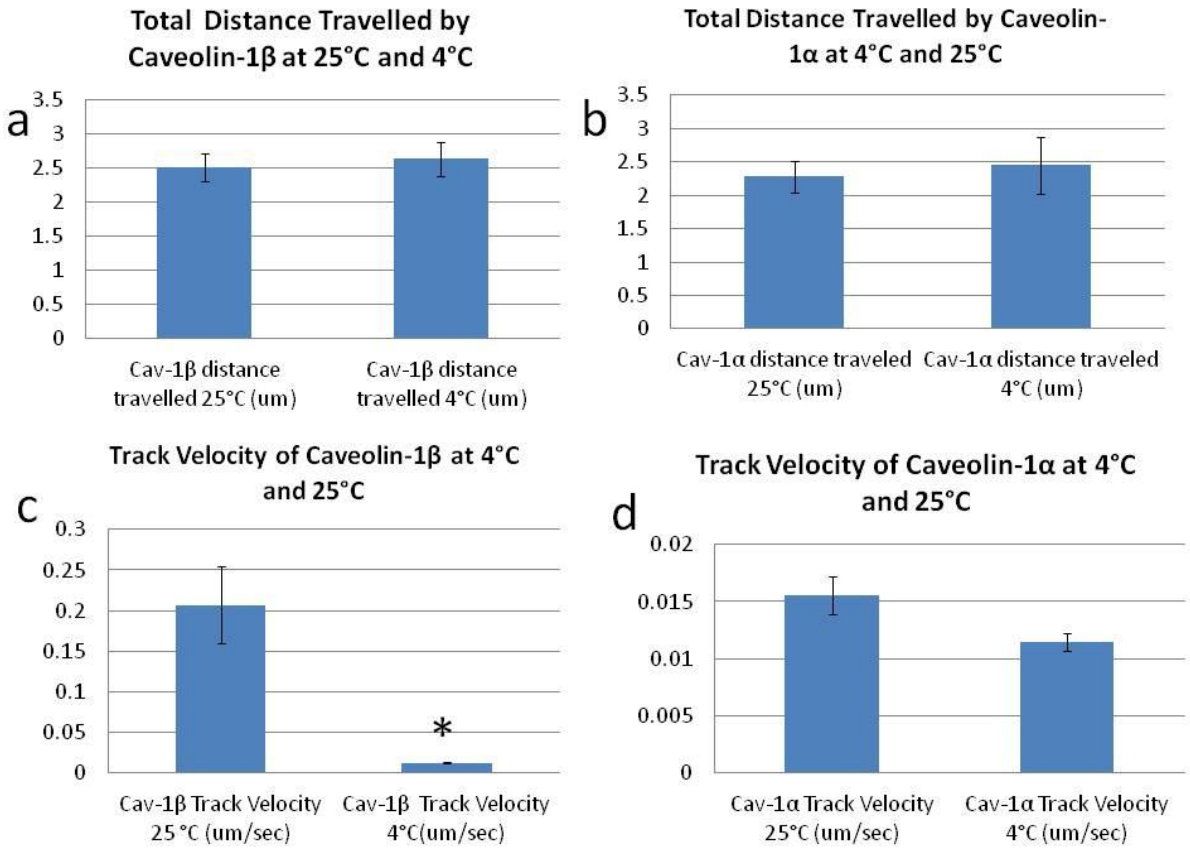


Figure 4.4 (a-b) The total distances travelled by caveolin-1α and caveolin-1β were calculated separately using Volocity software at 4°C and 25°C. (c-d). The track velocities of caveolin-1α and caveolin-1β were also calculated separately using the Volocity software. The asterisk represents statistical significance by a two tailed t-test (p value = 0.0076).

## Chapter 5

## DISCUSSION AND FUTURE WORK

The goal of this project was to determine if caveolae were mobile, what movement they engaged in, and to determine if caveolin-1α and caveolin-1β within the caveolae move at different rates. The steps to accomplishing these goals included taking time lapse photographs and analyzing data using the Volocity software and statistics. Similar to Keating et. al. experiments [9], it was found that the movements of caveolae are dynamic. It was also found that caveolin-1β was more dynamic than caveolin-1α. The results from my experiments agree with their findings.

Because we were able to quantify a track velocity for the caveolin proteins, this observation shows that they are not immobile micro-domains. The statistical significance in my results shows that caveolin-1β moves at a slower rate at 4°C, compared to at 25°C. This change in velocity in response to temperature change is in agreement with the Keating et. al. [9] findings that caveolin-1β is temperature-sensitive. Also, my experiments show that caveolin-1β moves statistically at a faster rate than caveolin-1α at 25°C. Like Keating et. al. [9] , caveolin-1α did not appear to be affected by the change in temperature. When comparing the track velocities and total distance travelled between caveolin-1β that was transfected alone, and caveolin-1β that was transfected with caveolin-1α, my results show that caveolin-1α may have an influence in the movement and speed of caveolin-1β. Future experiments should be done to interpret how one protein can influence the other. Although experiments could not be done at 37°C, based on the results, it could be predicted that the velocity of the clusters would higher at the increased temperature.

The calculated diffusion coefficients indicate that caveolin-1α and caveolin-1β are engaging anomalous diffusion and directed motion with diffusion. Based on the derived lines of best fit, the proteins that follow a power equation were the ones that engaged in anomalous diffusion. This finding means that the movement of the protein has a non-linear relationship with time [14]. The proteins that engage in directed motion with diffusion are experiencing drift at a certain velocity while they are diffusing [13]. The drift is denoted by the b*x* part of the equation of the polynomial line of best fit. Overall, my calculated diffusion coefficients did not coincide with Keating et. al. [9] coefficients for the same proteins. This may have been due to a smaller sample set in my data.

To gain further understanding of how the movement of caveolae is regulated by the cell, more experiments must be done. A few suggestions for future work may include investigating the influence of cholesterol on the movement of caveolae. This can be done by treating the cells with chemicals such as methyl-β-cyclodextrin, filipin or nystatin, which reduces the presence of cholesterol on the cell surface, and then calculating the velocity of caveolae via time lapse imaging. Another avenue to consider is the role of the cytoskeleton in caveolae movement. A possible experiment could be disrupting the association of caveolae to the cytoskeleton by down regulating the protein, filamin, an important protein for caveolae-cytoskeleton interaction in the cell [4]. With further experimentation, a better understanding of the dynamics of caveolae on the plasma membrane can be reached.

## REFERENCES


1. Parat, M.O., *The biology of caveolae: achievements and perspectives.* Int Rev Cell Mol Biol, 2009. **273**: p. 117-62.

2. Thomas, C.M. and E.J. Smart, *Caveolae structure and function.* J Cell Mol Med, 2008. **12**(3): p. 796-809.

3. Bastiani, M. and R.G. Parton, *Caveolae at a glance.* J Cell Sci. **123**(Pt 22): p. 3831-6.

4. Lajoie, P. and I.R. Nabi, *Lipid rafts, caveolae, and their endocytosis.* Int Rev Cell Mol Biol. **282**: p. 135-63.

5. Quest, A.F., J.L. Gutierrez-Pajares, and V.A. Torres, *Caveolin-1: an ambiguous partner in cell signalling and cancer.* J Cell Mol Med, 2008. **12**(4): p. 1130-50.

6. Nohe, A., Keating, E., Fivaz, M., Gisou van der Goot, F., and Peterson, N.O., *Dynamics and interaction of caveolin-1 isoforms with BMP-receptors.* J Cell Sci, 2005. **118**(Pt 3): p. 643-50.

7. Nohe, A., Keating, E., Loh, C., Underhill, M., and Peterson, N.O, *Caveolin-1 isoform reorganization studied by image correlation spectroscopy.* Faraday Discuss, 2004. **126**: p. 185-95; discussion 245-54.

8. Francesconi, A., R. Kumari, and R.S. Zukin, *Regulation of group I metabotropic glutamate receptor trafficking and signaling by the caveolar/lipid raft pathway.* J Neurosci, 2009. **29**(11): p. 3590-602.

9. Keating, E., A. Nohe, and N.O. Petersen, *Studies of distribution, location and dynamic properties of EGFR on the cell surface measured by image correlation spectroscopy.* Eur Biophys J, 2008. **37**(4): p. 469-81.

10. Chidlow, J.H., Jr. and W.C. Sessa, *Caveolae, caveolins, and cavins: complex control of cellular signalling and inflammation.* Cardiovasc Res. **86**(2): p. 219-25.

11. Hansen, C.G. and B.J. Nichols, *Molecular mechanisms of clathrin-independent endocytosis.* J Cell Sci, 2009. **122**(Pt 11): p. 1713-21.

12. Howes, M.T., S. Mayor, and R.G. Parton, *Molecules, mechanisms, and cellular roles of clathrin-independent endocytosis.* Curr Opin Cell Biol. **22**(4): p. 519-27.

13. Saxton, M.J., *Single-particle tracking: the distribution of diffusion coefficients.* Biophys J, 1997. **72**(4): p. 1744-53.

14. Malchus, N. and M. Weiss, *Elucidating anomalous protein diffusion in living cells with fluorescence correlation spectroscopy-facts and pitfalls.* J Fluoresc. **20**(1): p. 19-26.

## Appendix A

## RAW DATA

Table 1: Measured temperatures over duration of 60 minutes at 3 volts and 3 amps.

| 3.0 volts with the cap | | | | | | |
|---|---|---|---|---|---|---|
| Time (Minutes) | Temp (°F) | Temp (°F) | Temp (°F) | Temp (°F) | Average (°F) | Temp (°C) |
| 0 | 92 | 95 | 94 | 95 | 94 | 34.44444 |
| 5 | 102 | 94 | 92 | 94 | 95.5 | 35.27778 |
| 10 | 104 | 98 | 93 | 96 | 97.75 | 36.52778 |
| 15 | 104 | 98 | 95 | 97 | 98.5 | 36.94444 |
| 20 | 104 | 98 | 96 | 98 | 99 | 37.22222 |
| 25 | 104 | 98 | 96 | 98 | 99 | 37.22222 |
| 30 | 105 | 98 | 97 | 98 | 99.5 | 37.5 |
| 35 | 105 | 98 | 97 | 98 | 99.5 | 37.5 |
| 40 | 108 | 98 | 97 | 96 | 99.75 | 37.63889 |
| 45 | 109 | 100 | 96 | 98 | 100.75 | 38.19444 |
| 50 | 106 | 98 | 98 | 97 | 99.75 | 37.63889 |
| 55 | 106 | 98 | 98 | 98 | 100 | 37.77778 |
| 60 | 107 | 98 | 96 | 98 | 99.75 | 37.63889 |

Table 2: Measured temperatures over duration of 60 minutes at 2.9 volts and 3 amps.

| Time (minutes) | Temp (°F) | Temp (°F) | Average Temp (°F) | Temp( °C) |
|---|---|---|---|---|
| 0 | 77 | 93 | 85 | 29.44444 |
| 5 | 91 | 92 | 91.5 | 33.05556 |
| 10 | 95 | 95 | 95 | 35 |
| 15 | 95 | 95 | 95 | 35 |
| 20 | 97 | 96 | 96.5 | 35.83333 |
| 25 | 96 | 96 | 96 | 35.55556 |
| 30 | 95 | 98 | 96.5 | 35.83333 |
| 35 | 97 | 97 | 97 | 36.11111 |
| 40 | 97 | 97 | 97 | 36.11111 |
| 45 | | 97 | 97 | 36.11111 |
| 50 | 96 | 96 | 96 | 35.55556 |
| 55 | | 96 | 96 | 35.55556 |
| 60 | 97 | 97 | 97 | 36.11111 |

Table 3: Measured tempeatures over duration of 60 minutes at 2.4 volts and 3 amps.

| Time (minutes) | | Temperature (°F) | Temperature (°F) | Average Temp (°F) | Temperature (°C) |
|---|---|---|---|---|---|
| 0 | 97 | 93 | 95 | 95 | 35 |
| 5 | 93 | 96 | 95 | 94.66667 | 34.81481 |
| 10 | 93 | 98 | 98 | 96.33333 | 35.74074 |
| 15 | 94 | 99 | 99 | 97.33333 | 36.2963 |
| 20 | 95 | 99 | 99 | 97.66667 | 36.48148 |
| 25 | 95 | 99 | 103 | 99 | 37.22222 |
| 30 | 95 | 99 | 102 | 98.66667 | 37.03704 |
| 35 | 96 | 98 | 99 | 97.66667 | 36.48148 |
| 40 | 96 | 99 | 99 | 98 | 36.66667 |
| 45 | 96 | 98 | 102 | 98.66667 | 37.03704 |
| 50 | 96 | 98 | 99 | 97.66667 | 36.48148 |
| 55 | 96 | 98 | 100 | 98 | 36.66667 |
| 60 | 96 | 100 | 103 | 99.66667 | 37.59259 |

Table 4: Measured temperatures over duration of 60 minutes at 2.3 volts and 3 amps.

| Time(minutes) | Temp (°F) | Temp (°F) | Temp (°F) | Average (°F) | Temp(°C) |
|---|---|---|---|---|---|
| 0 | 94 | 94 | 95 | 94.33333 | 34.62963 |
| 5 | 95 | 90 | 94 | 93 | 33.88889 |
| 10 | 97 | 91 | 95 | 94.33333 | 34.62963 |
| 15 | 100 | 92 | 96 | 96 | 35.55556 |
| 20 | 97 | 93 | 96 | 95.33333 | 35.18519 |
| 25 | 97 | 94 | 96 | 95.66667 | 35.37037 |
| 30 | 97 | 95 | 96 | 96 | 35.55556 |
| 35 | 96 | 94 | 96 | 95.33333 | 35.18519 |
| 40 | 96 | 94 | 96 | 95.33333 | 35.18519 |
| 45 | 98 | 94 | 96 | 96 | 35.55556 |
| 50 | 97 | 95 | 98 | 96.66667 | 35.92593 |
| 55 | 97 | 94 | 98 | 96.33333 | 35.74074 |
| 60 | 97 | 95 | 97 | 96.33333 | 35.74074 |

Table 5: Measured tempeatures over duration of 60 minutes at 2.0 volts and 3 amps.

| Time (minutes) | Temperature (°F) | Tempeature (°C) |
|---|---|---|
| 0 | 95 | 35 |
| 5 | 96 | 35.55556 |
| 10 | 94 | 34.44444 |
| 15 | 94 | 34.44444 |
| 20 | 94 | 34.44444 |
| 25 | 95 | 35 |
| 30 | 96 | 35.55556 |
| 35 | 96 | 35.55556 |
| 40 | 95 | 35 |
| 45 | 96 | 35.55556 |
| 50 | 95 | 35 |
| 55 | 95 | 35 |
| 60 | 94 | 34.44444 |

Table 6: Average total distances travelled for caveolin-1α and caveolin-1β.

| | Caveolin-1β Transfected alone At 25°C (um) | Caveolin-1β 25°C Length (um) | Caveolin-1β 4°C length (um) | Caveolin-1α 25°C Length (um) | Caveolin-1α 4°C Length (um) |
|---|---|---|---|---|---|
| Average | 1.765655 | 2.514 | 2.635241379 | 2.279428571 | 2.4503 |
| Standard Deviation | 1.582551 | 1.627333293 | 1.37114021 | 1.414902123 | 1.335254037 |
| SEM | 0.293872 | 0.205024723 | 0.254614345 | 0.23916211 | 0.422244401 |
| N | 29 | 63 | 29 | 35 | 10 |

Table 7: Average track velocity of caveolin-1α and caveolin-1β

| | Caveolin-1β Transfected alone 25°C (um/sec) | Caveolin-1β 25°C Track Velocity (um/sec) | Caveolin-1β 4°C Track Velocity (um/sec) | Caveolin-1α 25°C Track Velocity (um/sec) | Caveolin-1α 4°C Track Velocity (um/sec) |
|---|---|---|---|---|---|
| Average | 0.019046 | 0.207123492 | 0.012969655 | 0.015549429 | 0.011504 |
| Standard Deviation | 0.02244 | 0.380251369 | 0.004323065 | 0.009776077 | 0.002468104 |
| SEM | 0.004167 | 0.047907169 | 0.000802773 | 0.001652459 | 0.000780483 |
| N | 29 | 63 | 29 | 35 | 10 |